Inhibition of aggregation of amyloid-β through covalent modification with benzylpenicillin; potential relevance to Alzheimer's disease

Izzeddin Alsalahat [a,b,*], Zubida M. Al-Majdoub [c], Mutasem O. Taha [d], Jill Barber [c], Harmesh Aojula [a], Nigel Hodson [e], Sally Freeman [a,**]

[a] Division of Pharmacy & Optometry, School of Health Sciences, Faculty of Biology, Medicine & Health, University of Manchester, Oxford Road, Manchester, M13 9PT, UK
[b] Department of Pharmaceutical Chemistry and Pharmacognosy, Faculty of Pharmacy, Applied Science Private University, Amman, 11931, Jordan
[c] Centre for Applied Pharmacokinetic Research, Division of Pharmacy & Optometry, School of Health Sciences, Faculty of Biology, Medicine & Health, University of Manchester, Oxford Road, Manchester, M13 9PT, UK
[d] Department of Pharmaceutical Sciences, Faculty of Pharmacy, University of Jordan, Jordan
[e] BioAFM Facility, Faculty of Biology, Medicine and Health, Stopford Building, University of Manchester, Oxford Road, Manchester, M13 9PT, UK

ARTICLE INFO

ABSTRACT

The pathogenesis of Alzheimer's disease (AD) is correlated with the misfolding and aggregation of amyloid-*beta* protein (Aβ). Here we report that the antibiotic benzylpenicillin (BP) can specifically bind to Aβ, modulate the process of aggregation and supress its cytotoxic effect, initially *via* a reversible binding interaction, followed by covalent bonding between specific functional groups (nucleophiles) within the Aβ peptide and the *beta*-lactam ring. Mass spectrometry and computational docking supported covalent modification of Aβ by BP. BP was found to inhibit aggregation of Aβ as revealed by the Thioflavin T (ThT) fluorescence assay and atomic force microscopy (AFM). In addition, BP treatment was found to have a cytoprotective activity against Aβ-induced cell cytotoxicity as shown by the 3-(4,5-dimethylthiazol-2-yl)-2,5-diphenyltetrazolium bromide (MTT) cell toxicity assay. The specific interaction of BP with Aβ suggests the possibility of structure-based drug design, leading to the identification of new drug candidates against AD. Moreover, good pharmacokinetics of *beta*-lactam antibiotics and safety on long-time use make them valuable candidates for drug repurposing towards neurological disorders such as AD.

1. Introduction

Alzheimer's disease (AD) is a neurodegenerative disease which results from progressive death of brain cells with subsequent loss of brain mass, leading to dementia and other behavioral changes [1]. Accumulation of aggregated proteins in fibrillar structures known as amyloid-*beta* (Aβ) is the key pathological hallmark of AD [2,3]. Aβ is a fragment of amyloid precursor protein (APP) [4], which under pathological conditions is sequentially cleaved by β-secretase and γ-secretase enzymes leading to the formation of extracellular Aβ proteins, mainly Aβ$_{(1-40)}$ and Aβ$_{(1-42)}$, as monomers [5]. The monomers aggregate to form soluble oligomers of Aβ strands and then β-sheets [6], which cumulatively form ordered fibrils known as β-plaques, a characteristic feature of AD [7].

The deposition of plaques onto the surface of brain cells leads to the deformation of the cell membrane and structure [8]. The soluble oligomers are believed to be the major contributing form with regards to AD pathogenesis and cytotoxicity [9]. The accumulation of plaques in the synapses leads to loss of communication between adjacent neurons and consequently to loss of signal transmission between connecting neurons [10].

Although targeting Aβ pathogenicity with small molecules is an

active area of research with promising *in vitro* activity, none of the drugs targeting Aβ have progressed to the clinical stage [11–13]. This is attributed to the ill-defined conformations of Aβ aggregation species and the fact that small molecules weakly bind nonspecifically to Aβ, ruling out structure-based drug design [14]. Several antibiotics have been reported to have a neuroprotective role in AD, including rifampicin [15–17], some tetracycline antibiotics [18,19], gramicidin S [20], D-cycloserine [21], amphotericin B [22] and doxorubicin [23]. Some forms of dementia have been linked to infectious conditions; notably syphilis, caused by infection with the spirochete bacterium, *Treponema pallidum*, which if untreated leads to severe changes in the brain. Positive effects of antibiotics such as penicillins on dementia have been documented, but are usually attributed to the prevention of microorganism entry into the brain, rather than to a direct action of antibiotics on Aβ [24–26].

In this study we investigated the ability of penicillins (specifically benzylpenicillin (BP)), to bind to Aβ through specific covalent modification and modulate Aβ aggregation, thereby suppressing toxicity.

2. Materials and methods

2.1. Materials and instrumentation

Ultra-pure recombinant $A\beta_{(1-40)}$ and $A\beta_{(1-42)}$ were purchased from rPeptide (UK). $A\beta_{(1-28)}$ was purchased from Bachem (Germany). 1,1,1,3,3,3-Hexafluoroisopropanol (HFIP) (99.8% GC) was purchased from Fluka. Distilled trifluoracetic acid (TFA) (Molecular Biology grade), Dulbecco A PBS buffer (320 mM NaCl, 6 mM KCl, 16 mM Na_2HPO_4 and 2 mM KH_2PO_4, at pH 7.4) and ThT (Molecular Biology grade) were purchased from Sigma-Aldrich. The SH-SY5Y cells were obtained from ATCC and plated in 96-well polystyrene plates purchased from Thermo-Fisher Scientific (UK). Glycine buffer was purchased from Thermo-Fisher Scientific (UK). 96-well black-bottomed microplates were purchased from Berthold (UK).

Mica (Muscovite mica, 9.5 mm diameter, 0.15–0.21 mm thickness) was purchased from Agar Scientific (UK). Samples were imaged in air in ScanAsyst™ mode using a Bruker Multimode AFM with a Nanoscope V controller and a "J" scanner (Bruker UK Ltd., Coventry, UK). Imaging was performed using ScanAsyst-Air probes with nominal spring constant of 0.4 N/m (Bruker AXS S.A.S, France), and the system was controlled via the Bruker Nanoscope software (v8.15).

2.2. Sample preparation of Aβ peptide

Disaggregation of pre-formed Aβ fibrils was achieved by using TFA and HFIP. First, neat TFA was added to an Aβ sample in a 1:1 (mg/ml) ratio. The samples were vortexed and sonicated for 15 min, during which an additional 1.0 ml of TFA was added. Complete dissolution was checked after centrifugation. TFA was removed by dry N_2 gas and residual traces of TFA were further removed by adding HFIP at a concentration of 10 mM and evaporating it with a stream of dry N_2 gas three times. HFIP traces were removed under vacuum (0.5 mm Hg, 2 h) or by freeze-drying [27,28]. Peptide concentrations were calculated using the extinction coefficients of phenylalanine (molar extinction coefficient of 197 M^{-1} cm^{-1} at 257.4 nm) [29].

2.3. 3-(4,5-Dimethylthiazol-2-yl)-2,5-diphenyltetrazolium bromide (MTT) cell toxicity assay

SH-SY5Y cell viability was tested using the trypan blue method described by Field and coworkers [30]. The optimal cell density for the experiments was determined by plating cells at different concentrations for 48 and 72 h. BP was tested on cells without the peptide, before testing BP in the presence of $A\beta_{(1-42)}$ at a molar ratio of 1:5 ($A\beta_{(1-42)}$: BP), according to the ATCC guidelines and [29,31], as described in the supplementary data.

2.4. Thioflavin T (ThT) aggregation inhibition assay

The ThT fluorescence assay was performed using freeze-dried disaggregated stocks of $A\beta_{(1-42)}$, so that solutions of a concentration of 100 μM of $A\beta_{(1-42)}$, with or without BP at a 1:10 M ratio, $A\beta_{(1-42)}$: BP were prepared. $A\beta_{(1-42)}$ was dissolved to a concentration of 20 mM in DMSO and then diluted using sterile-filtered Milli-Q water to 200 μM [29]. BP was dissolved in DMSO so that the final concentration was 0.5% (v/v), and then diluted to 2 mM using sterile-filtered 2 x Dulbecco A PBS buffer and thoroughly vortexed until dissolution. After that, a 250 μL aliquot of $A\beta_{(1-42)}$ solution was added to a 250 μL aliquot of BP to give a total assay volume of 500 μL containing 100 μM $A\beta_{(1-42)}$ and 500 μM of BP in 1 x Dulbecco PBS buffer. The assay mixture was vortexed and kept at 37 °C for 4 days and the aggregation was monitored by the ThT fluorescence assay [29].

The ThT stock solution at a concentration of 500 μM was prepared in 50 mM glycine buffer at pH 8.5. Aliquots of 1.0 ml of ThT stock solution in glycine buffer were kept frozen, when needed they were allowed to thaw and diluted to 20 μM ThT in glycine buffer. Samples were thoroughly vortexed and a quantity of 20 μL of each sample for each repeat was added to each well containing 180 μL of the ThT solution. The fluorescence was measured in a Twinkle LB970 Fluorescence Plate Reader (Berthold Technologies) using excitation and emission filters F440-StorA3 and F495-StorA3, respectively, with lamp intensity set at 10000 and 3 s "shake" step prior to reading. Samples were tested in triplicate and ThT fluorescence readings were recorded at 24, 48, 72 and 96 h intervals [29].

2.5. Atomic force microscopy (AFM)

The $A\beta_{(1-42)}$ test samples were prepared as described in the ThT assay protocols [29] and incubated for 5 days. Studying amyloid aggregation with AFM has been previously described [32,33]. Briefly, 25 μL of sample was deposited onto a freshly cleaved mica for 20 min and were then washed with 2 ml of 0.22 μm-filtered double distilled water (applied in aliquots of approx. 200 μl) to remove any salts or unadsorbed protein, prior to drying at room temperature. Height, Peak-Force Error and Inphase images with scan sizes of either 2 μm^2 or 5 μm^2 were captured at a scan rate of 1 Hz and at a relative humidity of <50%. Data was first-order flattened prior to analysis using the Nanoscope Analysis software (v1.5).

2.6. Mass spectrometry

Solutions of 100 μM $A\beta_{(1-40)}$ and $A\beta_{(1-28)}$ peptides prepared in 50 mM PBS from lyophilized disaggregated stocks were incubated with or without 500 μM BP at 37 °C for 24 h. Samples containing intact $A\beta_{(1-40)}$ peptides were analyzed by MALDI-time-of-flight mass spectrometry (MALDI-TOF MS). Samples containing $A\beta_{(1-28)}$, digested $A\beta_{(1-40)}$ and amino acids were analyzed by electrospray ionization mass spectrometry (ESI MS) as direct infusion or LC-ESI MS.

Samples of $A\beta_{(1-40)}$ incubated with or without BP were digested by endoproteinase Glu-C enzyme according to the manufacturer's protocols. For Glu-C digestion, a ratio of 1:60 (w/w) of enzyme to substrate was used. The pH was adjusted to 7.4 and the samples were incubated overnight at 37 °C. All the samples were desalted using C18 Zip-Tip TM (Millipore, Billerica, MA) prior to MS analysis (direct infusion, LC-MS and LC-MS/MS) mass spectrometry.

MALDI-TOF MS: The matrix used was 2,5-dihydroxybenzoic acid (DHB). A saturated solution of DHB was made by dissolving 15 mg in 70% ACN in 0.1% TFA (1 ml). The solution was vortexed and centrifuged at 6000 rpm for 3 min. The supernatant was collected and the samples were mixed with the matrix in a 1:2 ratio in a microcentrifuge tube. The mixtures were then placed on a polished steel MALDI target (MTP 384, Bruker, Germany), left to dry and subsequently analyzed by MALDI-TOF MS. The machine was externally calibrated before each
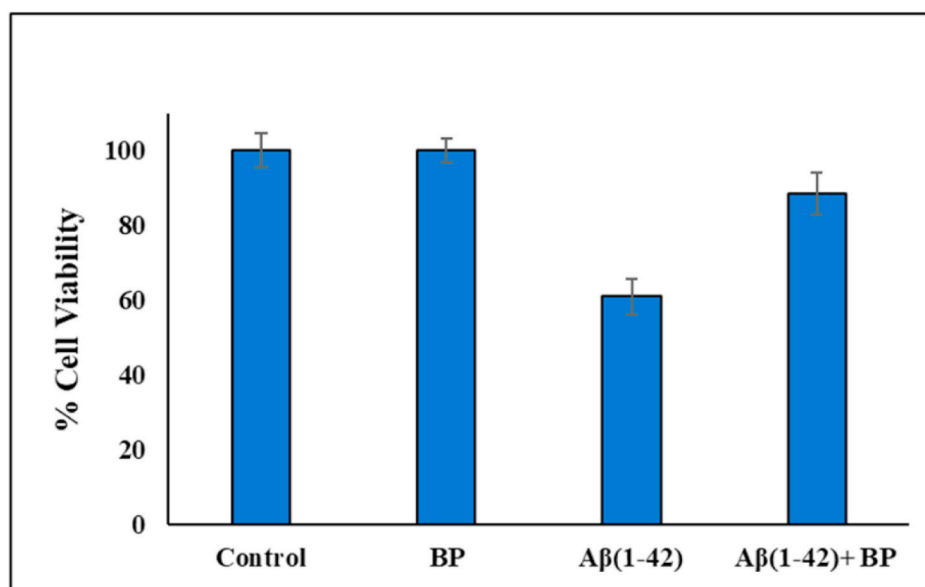
Fig. 1. Viability of SH-SY5Y cells after treatment with BP (100 μM) alone, $A\beta_{(1-42)}$ (20 μM) alone or with $A\beta_{(1-42)}$ (20 μM) and BP (100 μM). Control sample contained the cells in media only. (p-value < 0.05).

acquisition by QCAL [34] or Protein Calibration Standard I (Bruker, Germany). MALDI-TOF experiments were performed using an Ultraflex II (Bruker, Bremen, Germany) instrument. The spectra were acquired in linear mode for positive ions over a range of m/z 700–10000 with ion suppression below m/z 650. Laser shots were fired at 200 Hz with an average of 500 laser shots, and 10 spectra were accumulated. The laser attenuator was set to 64%, with a laser range set to 20% and a surface area set to large. Data acquisition was performed using FlexControlTM Version 3.0 (Bruker, Germany) and analysis was performed using Flex-Analysis software.

ESI MS: Samples containing digested $A\beta_{(1-40)}$ and amino acids were analyzed by LC-MS and direct infusion mass spectrometry (DIMS) using Q-TOF Global (Waters, UK). LC-MS/MS analyses were conducted using an Ultimate 3000 LC system (Dionex, CA) connected in-line to a Q-TOF Global mass spectrometer (Waters, UK). Samples of $A\beta_{(1-40)}$ incubated with and without BP, and digested with Glu-C were injected onto an Ultimate 3000 LC system (Dionex) with mobile phases A (2% acetonitrile and 0.1% formic acid) and B (95% acetonitrile and 0.1% formic acid). Peptides were eluted from an Acclaim Pepmap 75 μm × 15 cm, C18 analytical column (LC Packings, USA) with a gradient of 10–50% buffer B over 45 min at a flow rate of 200 nL min^{-1}. MS and MS/MS data were collected with a Global Q-TOF mass spectrometer (Waters, U.K.) for the ranges of m/z 400–1800 and m/z 50–1800, respectively. The LC system was connected to Q-TOF Global through a distal-coated fused silica PicoTip emitter (New Objective, Inc., USA) using a capillary voltage of 2.0–2.8 kV into a Z-sprayTM ion source.

DIMS: Samples containing $A\beta_{(1-28)}$ were analyzed using a Synapt G2 mass spectrometer (Waters, UK), equipped with an electrospray ion (ESI) source, hybrid quadrupole, ion mobility device and orthogonal time-of-flight (TOF) analyzer, and calibrated with aqueous cesium iodide (CsI) cluster ions according to the manufacturer's guidelines. Samples containing $A\beta_{(1-28)}$ peptide with or without BP (1 μg/μl) were directly infused using a fused silica PicoTip™ emitter (New Objective, Inc., MA, USA) at a flow rate of 0.1 ml min^{-1} using capillary voltage, cone voltage and extracted voltage at 2.0 kV, 30 V and 2.5 V, respectively. Nitrogen was used as a desolvation gas at a pressure of 0.8 p. s.i. (55.16 mbar). The source temperature was set to 60 °C and backing pressure at 2 mbar. The instrument control, data acquisition and processing were performed using MassLynx 4.1 (Waters, UK). TOF-MS data were acquired in continuum mode over the range m/z 100–2000.

2.7. Molecular docking

The 3D coordinates of solution structure of $A\beta_{(1-42)}$ were retrieved from the Protein Data Bank (PDB code: 1IYT). However, 1IYT includes 10 conformers and in order to select the best conformer the single point energy was calculated for each conformer implementing CHARMm forced field and generalized Born model (Born radii calculated by integration of molecular volume) to simulate solvation water effects [35]. The most stable conformer (of least calculated energy $= -869.0$ kcal/mol) was selected for the docking study without further energy minimization.

To identify the best docking site within $A\beta_{(1-42)}$, BP was docked into cavities across the peptide surface. The best docking energy score converged upon docking BP into the peptide chain corresponding to the first 5 amino acids (Asp1-Ala 2-Glu3-Phe4-Arg5).

CDOCKER is a CHARMm-based simulated annealing/molecular dynamics method that uses rigid receptor for docking [36]. CDOCKER protocol includes the following steps. (i) A set of ligand conformations are generated using high-temperature molecular dynamics starting with different random seeds. (ii) Random orientations of the conformations are produced by translating the centre of the ligand to a specified location within the receptor active site, and performing a series of random rotations. (iii) A softened energy is calculated and the orientation is kept if the energy is less than a specified threshold. This process continues until either the desired number of low-energy orientations is found, or the maximum number of bad orientations has been tried. (iv) Each orientation is subjected to simulated annealing molecular dynamics. The temperature is heated up to a high pre-set temperature then cooled to the target temperature. (v) A final minimization of the ligand in the rigid receptor using non-softened potential is performed. For each final pose, the CHARMm energy (interaction energy plus ligand strain) and the interaction energy alone are calculated. The poses are sorted by CHARMm energy and the top scoring (most negative, thus favourable to binding) poses are retained. To enhance performance and shorten calculation times, nonbond energy grid is used for interaction energy calculations, rather than the full potential energy terms usually used by CHARMm.

The following CDOCKER parameters were implemented in the presented project: (i) Starting ligands' conformers were energy-minimized then heated to 1000 K over 1000 molecular dynamics steps (these include heating and equilibration phases) to generate 10 random
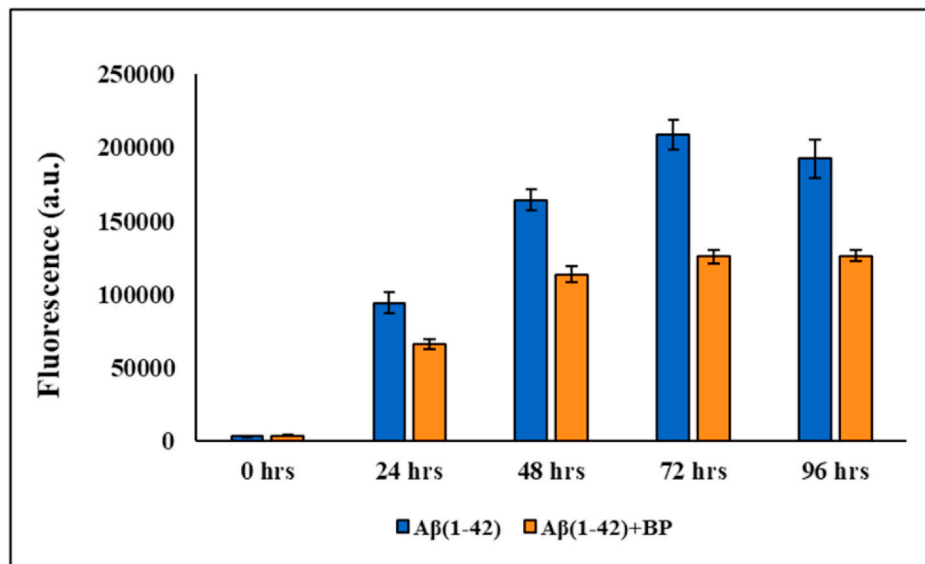
Fig. 2. ThT assay of Aβ$_{(1-42)}$ aggregation inhibition by BP, incubated at a 1:10 M ratio (Aβ$_{(1-42)}$: BP) for 96 h.

starting conformations for each ligand. (ii) Each random conformer was rotated 10 times within the binding pocket for subsequent energy refinement. The van der Waals energies of the resulting conformers/poses were evaluated and those of ≥ 300 kcal/mol were discarded. (iii) Remaining conformers/poses were exposed to a cycle of simulated annealing over 2000 heating steps to targeted temperature of 700 K followed by 5000 cooling steps to targeted temperature of 300 K. (iv) The docked poses were energy minimized to a final minimization gradient tolerance zero Kcal/mol/Å. (v) Top 10 poses were saved for subsequent scoring. (vi) The resulting poses were scored by CDOCKER Energy and the pose that achieved the highest score was selected for analysis.

3. Results and discussion

3.1. MTT cell toxicity assay

The human-derived neuroblastoma SH-SY5Y cell line is often used as
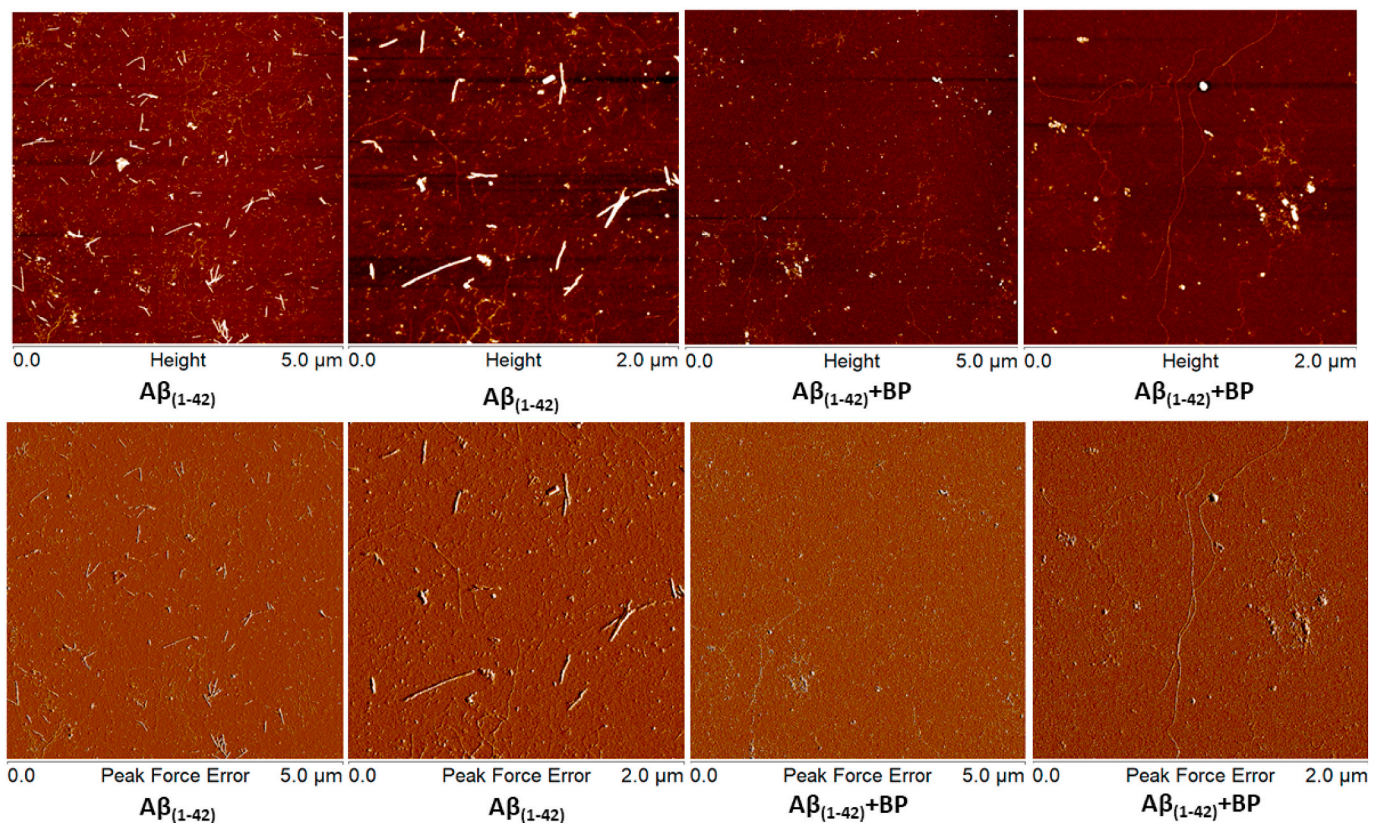
Fig. 3. AFM height images (top panel) and peak force error images (bottom panel) in ScanAsyst mode showing the effect of BP on Aβ$_{(1-42)}$ aggregation after incubation for 5 days. Each image is shown at 2- and 5-μm resolution.
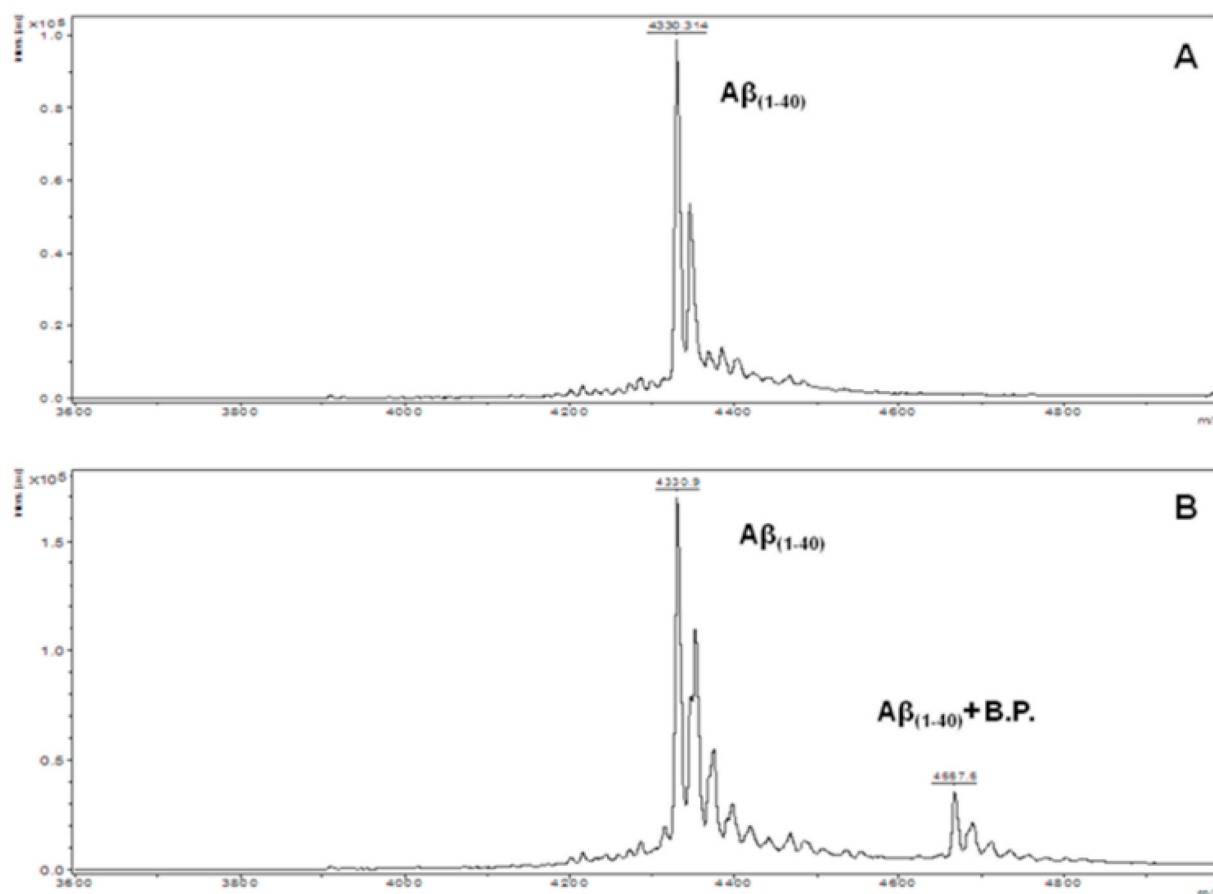
Fig. 4. MALDI-TOF mass spectra (in linear mode) of (A) Aβ$_{(1-40)}$ without BP, and (B) Aβ$_{(1-40)}$ with BP, incubated under physiological conditions for 24 h. The peak (~4668 Da) corresponds to the adduct of BP and Aβ$_{(1-40)}$.

an *in vitro* neural model for evaluating Aβ induced toxicity. The toxic effect of Aβ$_{(1-42)}$ peptide and BP on this cell line, and the ability of BP to inhibit Aβ$_{(1-42)}$ cell toxicity was assessed by measuring the reduction of MTT. The cell density for the following experiments was 1×10^5 cells/mL and the incubation time was 72 h. BP was tested at different concentrations for any possible toxic effects on the SH-SY5Y cell line, with no toxic effect observed at 100 μM (Fig. 1).

The effect of BP on Aβ$_{(1-42)}$- induced cell toxicity was then tested on SH-SY5Y cells at a 1:5 ratio (Aβ$_{(1-42)}$ peptide to BP) by measuring the reduction of MTT dye. In the absence of BP, the percentage cell viability after exposure to Aβ$_{(1-42)}$ was approximately 60%, compared to the control with the cells in the media only (Fig. 1). BP showed considerable cell protection against Aβ$_{(1-42)}$- induced cell toxicity, reverting the viability to ~89%. Having shown that BP could significantly reduce Aβ$_{(1-42)}$- induced cell toxicity, its interaction with Aβ$_{(1-42)}$ was evaluated.

3.2. Thioflavin T (ThT) fluorescence assay

The ThT fluorescence assay measures the change in fluorescence of ThT dye after binding to amyloid aggregates, with an increase in fluorescence intensity indicated by an increase in Aβ aggregation [37]. In the literature, the anti-aggregating activity of compounds was tested at a range of molar ratios: 5-fold [38], 10-fold [29,39,40] or 20-fold [41] molar excess when compared with Aβ$_{(1-40)}$ or Aβ$_{(1-42)}$. Here BP was tested for its ability to inhibit the aggregation of Aβ$_{(1-42)}$ over 96 h at a 1:10 M ratio (Aβ$_{(1-42)}$: BP), which is within the ratios reported in the literature (Fig. 2).

The spectroscopic range of activity of ThT is within 450 and 482 nm [42], whereas penicillins have negligible absorption above 400 nM and

therefore do not interfere with the ThT assay [43]. To confirm that the fluorescence measured is indeed due to the presence of fibrils, the ThT signal was corrected by subtracting the ThT fluorescence of the BP/PBS control sample from the ThT fluorescence of the Aβ-BP mixture, and the ThT fluorescence of the negative control (containing only PBS) from the ThT fluorescence of the Aβ alone.

For Aβ$_{(1-42)}$ control samples, Aβ aggregation increased with the time of incubation, as reflected by the increase in ThT fluorescence intensity. For Aβ$_{(1-42)}$ samples incubated with BP, the ThT fluorescence intensity increased over the period of incubation but at a significantly lower rate compared with the Aβ$_{(1-42)}$ control samples. In fact, no further significant increase in aggregation was observed after 48 h. As BP was found to slow and then arrest the aggregation of Aβ$_{(1-42)}$ over the period of incubation, the ThT assay was followed by studying the morphology of Aβ aggregates by AFM.

3.3. Atomic force microscopy (AFM) studies

The morphology of the Aβ aggregates was studied using atomic force microscopy (AFM) with ScanAsyst technology, which allowed automatic image optimization. Aβ$_{(1-42)}$ samples with and without BP were incubated at room temperature for 5 days. For the Aβ$_{(1-42)}$ samples without BP, AFM revealed the presence of fibrillar aggregates up to 35 nm in width and 128 nm in length (Fig. 3). Protofibrils and globular aggregates were also observed.

AFM revealed the presence of fibrillar aggregates and protofibrils in the Aβ$_{(1-42)}$ samples without BP. Fibrils can be formed directly from accumulation of unstructured monomers, unstructured paranuclei, large oligomers, or through a linear conversion from monomers, paranuclei, oligomers, protofibrils and then fibrils. With time, the globular
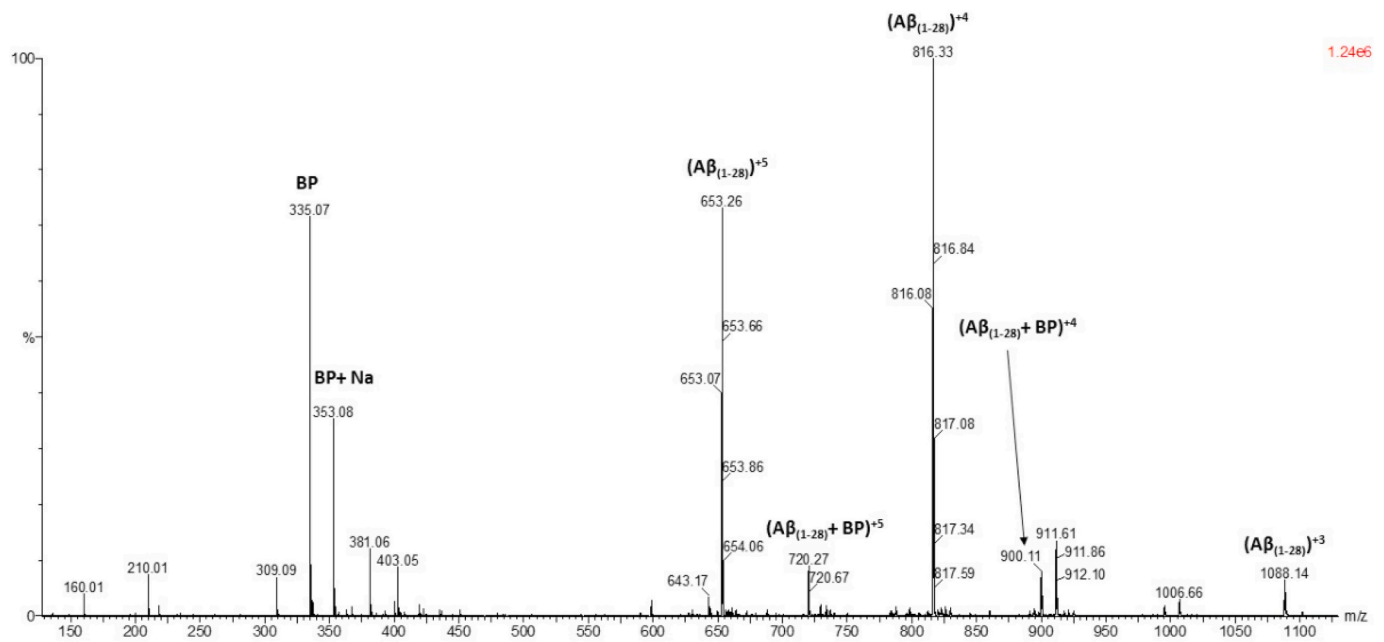
Fig. 5. ESI-MS of Aβ$_{(1-28)}$ incubated with BP. The peaks at m/z 900.11 and m/z 720.27 correspond to (Aβ$_{(1-28)}$ + BP)$^{+5}$ and (Aβ$_{(1-28)}$ + BP)$^{+4}$, respectively.

aggregates assemble and associate into linear protofibrils [44–46].

For Aβ samples incubated with BP, aggregation was significantly lower, with the presence of limited amount of thinner winding proto-fibrils compared to the Aβ$_{(1-42)}$ samples. Also, small, medium size and globular aggregates were present. This confirms that BP has an inhibitory effect on Aβ aggregation, which is consistent with the ThT fluorescence data.

3.4. Mass spectrometry

MALDI-TOF and ESI mass spectrometry techniques were used to study the hypothesized covalent interaction between Aβ and BP, as a model compound for a *beta*-lactam moiety. It was proposed that modulation of Aβ peptide aggregation could involve a nucleophilic interaction between the hydroxyl groups of the serine residues, the ε-amino groups of the lysine residues or the N-terminus amino group in Aβ peptide, with the *beta*-lactam moiety of BP. To probe this potential interaction, BP was incubated with Aβ$_{(1-40)}$ for 24 h under physiological conditions. The MALDI mass spectrum of Aβ$_{(1-40)}$ alone incubated for

24 h (Fig. 4 A) showed a peak corresponding to the MH$^+$ ion at 4330 Da. In the presence of BP, a peak at 4668 Da corresponding to its adduct with Aβ$_{(1-40)}$ was observed (Fig. 4 B).

To exclude the effect of Aβ aggregation on covalent adduct formation, BP was incubated with the more soluble and less aggregating Aβ$_{(1-28)}$ peptide and analyzed using ESI mass spectrometry. The ESI spectrum of Aβ$_{(1-28)}$ incubated with BP confirms adduct formation between Aβ$_{(1-28)}$ and one molecule of BP (Fig. 5), where the peaks at m/z 900.11 and m/z 720.27 correspond to (Aβ$_{(1-28)}$+BP)$^{+5}$ and (Aβ$_{(1-28)}$+BP)$^{+4}$, respectively.

In order to determine the target moieties of BP in Aβ, the reaction mixture of Aβ$_{(1-40)}$ and BP was digested by endopeptidase Glu-C and analyzed by mass spectrometry (LC-MS and LC-MS/MS). Glu-C cleaves peptide bonds at the carboxyl side of glutamyl (E) and aspartyl (D) amino acids in phosphate buffer at pH 7.8. The monoisotopic and the average m/z values of the possible fragments produced after digestion by Glu-C enzyme were calculated by the aid of Protein Prospector website (prospector.ucsf.edu). Three missed cleavages were allowed [47] (See Table 1 in supplementary data).
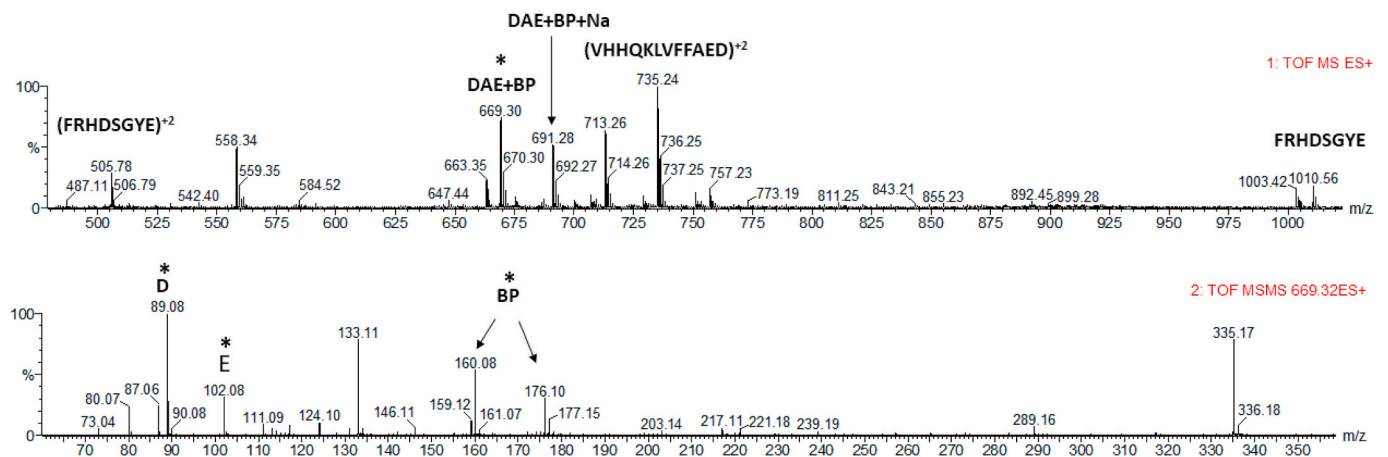
Fig. 6. ESI-MS (above) and ESI-MS/MS (below) of the adduct formed between the DAE fragment and BP. The peaks at m/z 669.30 and m/z 691.28 correspond to the DAE fragment bound to BP and its sodiated ion, respectively. The peaks at m/z 102.08 and 89.08 correspond to decarboxylated glutamic acid (E) and aspartic acid (D), respectively. The peaks at m/z 160.08 and 176.10 are the major two fragments of BP.
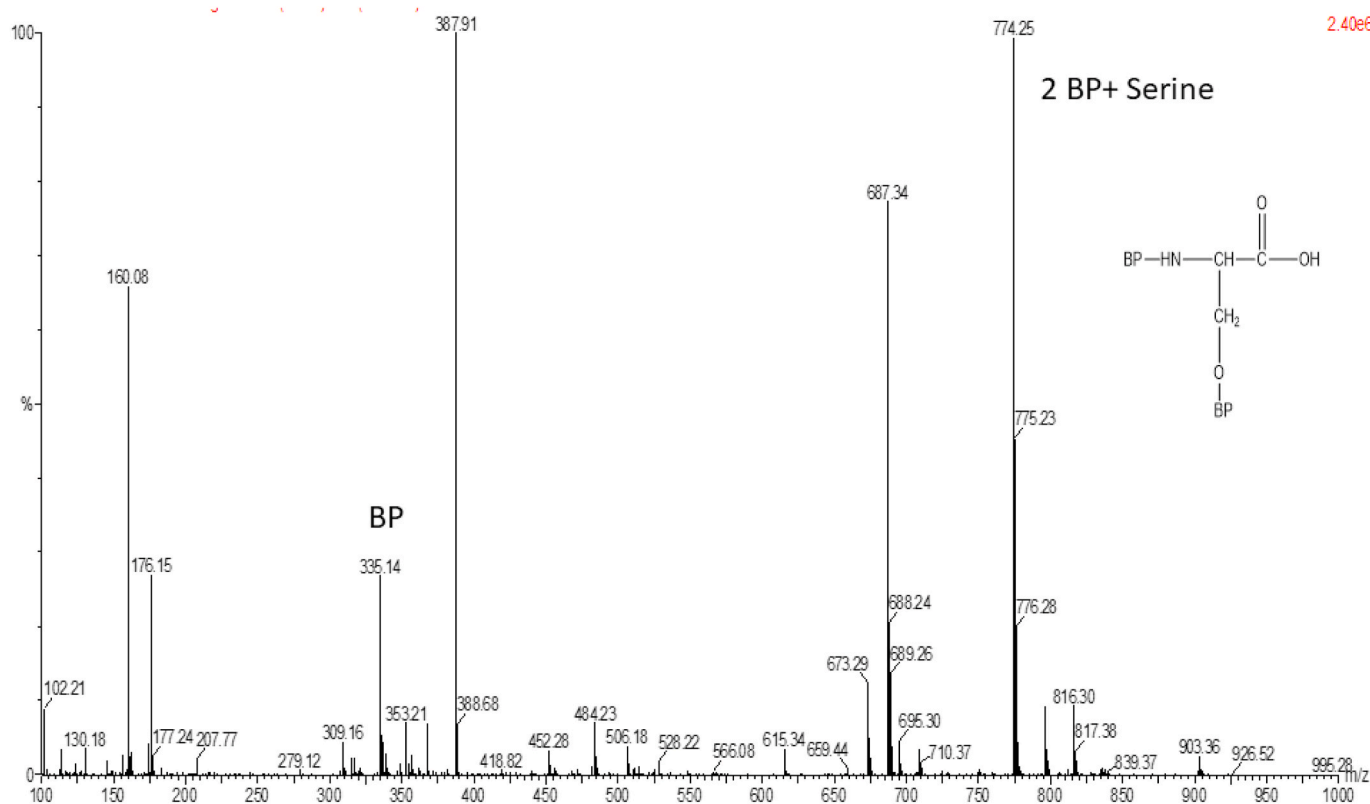
Fig. 7. LC-MS spectrum of serine incubated with BP. The peak m/z 774.25 corresponds to the adduct of serine with two molecules of BP.
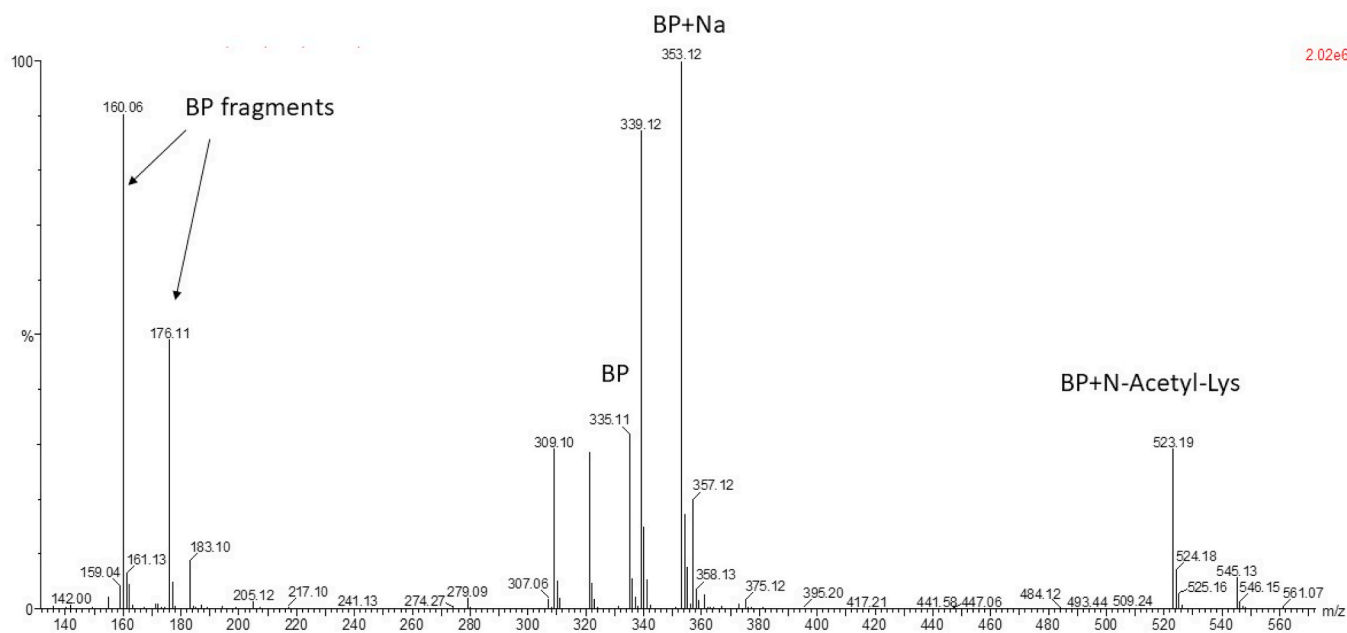
Fig. 8. LC-MS spectrum of N-acetyl-lysine incubated with BP. The peak m/z 523.22 corresponds to the adduct formed between BP and N-acetyl-lysine.

A peak corresponding to the fragment m/z 1325 (DAEFRHDSGYE) bound to BP as a doubly charged ion at m/z 830 was found (see Fig. 1 in supplementary data). However, this peak could not be resolved in the LC-MS/MS spectra to characterize its sequence, possibly because the formed bond could not withstand the high fragmentation energy of Tandem MS/MS. A peak corresponding to an adduct between the fragment DAE and BP at 669.30 m/z was also detected (Fig. 6). In ESI-MS/MS, the fragmentation products of DAE and BP adduct were also resolved.

Only a single BP molecule interacted with the Aβ peptide, even though there are five nucleophiles (the N-terminal amino group, two serine hydroxyl groups and two lysine ε-amino residues). This is not surprising as complex biomolecules often strongly favour one nucleophile when a range are available. This is seen in proteins, in which lysine nucleophiles are often favoured for reaction with inflexible drug molecules, such as erythromycin [48]. To address the issue that the
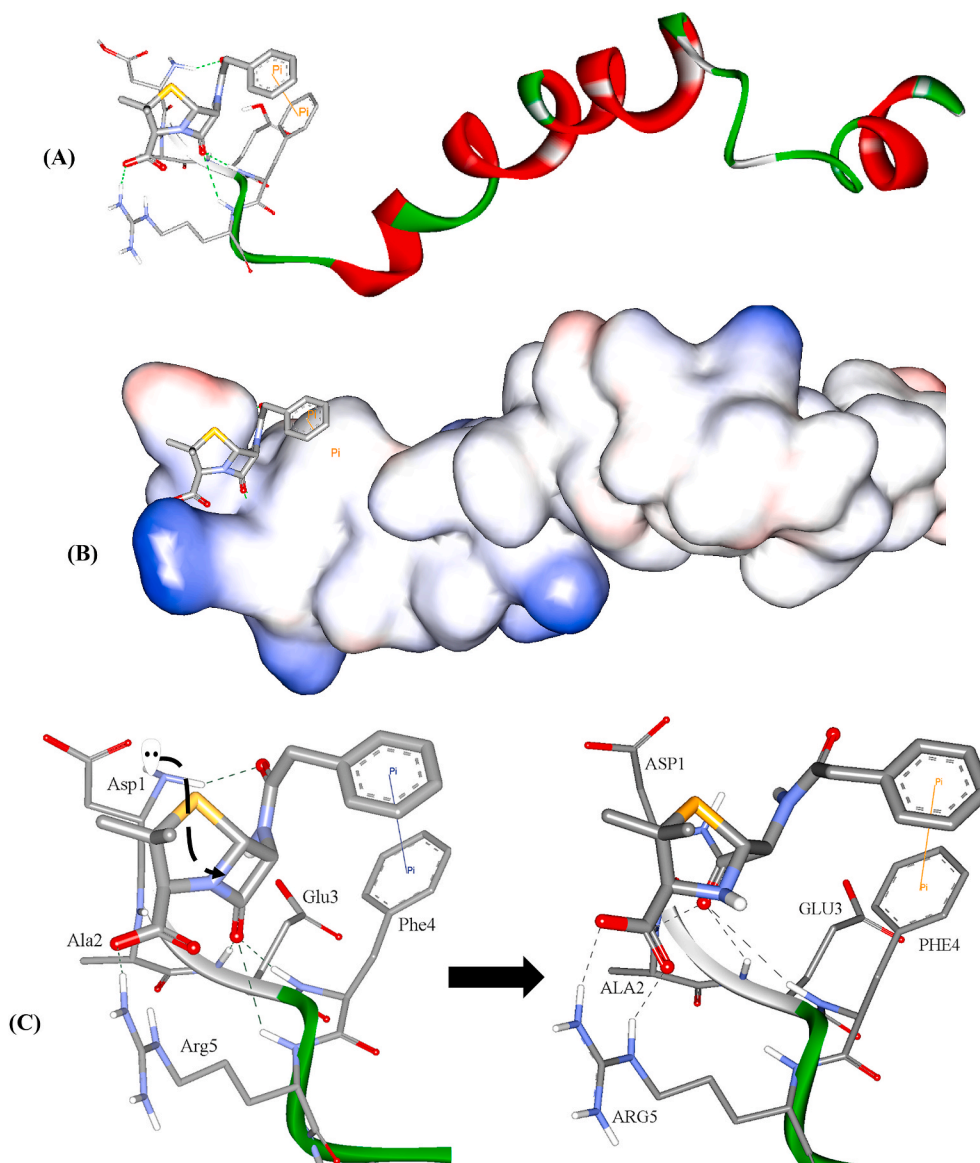
Fig. 9. BP docked into Aβ$_{(1-42)}$ (PDB code 1IYT). (A) and (B) show the panoramic views of the docked pose with and without molecular surface covering the peptide, respectively. (C) shows the detailed reversible attractive interactions anchoring BP and the proposed nucleophilic attack of the terminal amine of Asp1 on the β-lactam ring of BP.

nucleophile had not definitively been identified, BP was incubated with serine (which has a free N-terminus and a free hydroxyl group) and N-acetyl-lysine (which has a free ε-amino group) under the same conditions. As shown in Fig. 7, a peak corresponding to an adduct formed between serine and two molecules of BP was detected at *m/z* 774. Additionally, incubation of BP with N-acetyl-lysine shows that the ε-amino moiety is a potential target for BP (Fig. 8).

Thus, although it is clear that BP binds to Aβ$_{(1-28)}$ and Aβ$_{(1-42)}$ under mild conditions in a 1:1 stoichiometry, these experiments do not confirm which nucleophile is utilised in the reaction. Adduct formation appears to have protective effects against aggregation of Aβ, the process characteristic of Alzheimer's Disease.

3.5. Molecular docking

To consider the atomic details of the BP-amyloid interaction, computational docking of BP to the solution structure of Aβ$_{(1-42)}$ (PDB code 1IYT) was performed [49]. Interestingly, the top-ranking BP poses converged around residues Asp1 to Arg5 of Aβ (Fig. 9 A and B), which

confirms the results obtained by mass spectrometry on the full-length Aβ. Inspection of the components contributing to the total docking score of the top-ranked poses, showed a predominance of polar hydrogen-bonding interactions over non-polar interactions. In these poses, H-bonding interactions were found to take place between the amide carbonyl oxygen of BP and the terminal amino group of Asp1, and the *beta*-lactam carbonyl oxygen of BP with the peptide backbone NH groups of Ala 2 (Fig. 9 C). These interactions increase the nucleophilicity of the terminal amino group and the susceptibility towards a nucleophilic attack at the carbonyl carbon of the *beta*-lactam ring in BP. Also, a hydrogen-bond was found between Glu 4, Phe4 and Arg5, and the carbonyl and hydroxyl oxygen atoms of the carboxylic group of BP with the guanidino group of Arg5. In addition, a π-stacking interaction between the aromatic rings of BP and Phe4 is observed (Fig. 9 C).

Although all the nucleophilic groups in Aβ were shown to be targets for BP, molecular docking and MS studies (the following section) on the full-length Aβ showed that the terminal amino group of Aβ is more favourable for the proposed nucleophilic interaction with BP. The ligand is predicted *via* these docking calculations to prefer the general

Fig. 10. The proposed mechanism of interaction of Aβ and BP. This interaction of Aβ and BP involves the hydroxyl and amino moieties of Aβ to give amide A and ester B.

proximity of the terminal amino group of Aβ which is in agreement with the MS studies of the full-length Aβ that confirmed the interaction between BP and Aβ through the N-terminal amino group.

4. Conclusion

The neuroprotective role of antibiotics was first reported by Chui and co-workers [50], as prevalence of dementia was significantly decreased in leprosy patients who received long-term treatment with antibiotics. Several antibiotics (listed in the introduction) were reported to have a neuroprotective role in neurodegenerative diseases such AD. Many antibiotics can cross the blood-brain barrier (BBB) and have been used for a long time without serious toxic effects [51]. Furthermore, some antibiotics including the *beta*-lactam antibiotic ceftriaxone [52], were reported to exhibit antioxidant and strong anti-inflammatory properties, which can be of value in neurodegenerative disease. Antibiotics as multi-target molecules with anti-oxidant, anti-inflammatory and protein disaggregation properties constitute a promising approach for tackling neurodegenerative diseases such as AD. Several clinical studies reported that treatment with antibiotics at sub-antimicrobial doses do not affect the native human microbiota [53,54] even when used long-term [53,55, 56], or lead to the emergence of antibiotic resistance [53,54]. Oral antibiotics capable of reaching the brain at protective levels, without affecting microbiota, can be of value in halting the formation of toxic amyloid species [51].

The specific interaction of Aβ with BP suggests the possibility of structure-based drug design, leading to the identification of new drug candidates against AD. Moreover, the good pharmacokinetics of *beta*-lactam antibiotics and safety of long-term use make them valuable candidates for potential drug repurposing towards AD.

Despite the structural diversity of the anti-aggregation antibiotics, it has been suggested that some of these small molecules target a common structural arrangement in Aβ. Structural analysis of these molecules infers the prevalence of the motif O═CCCOH (as in the tetracyclines doxycycline and minocycline, amphotericin B and rifampicin) or O═CCNH (as in D-cycloserine and gramicidine S). The O═CCNH motif

is also present in BP, which constitutes a hydrogen bond donor/acceptor pair arrangement that interacts with a parallel motif in the Aβ protein backbone [51,57,58]. Also, as suggested by the 3D-QSAR computational analysis, the presence of aromatic rings in the antibiotics mediate π-stacking interactions with Aβ (such as Phe4), which is associated with their anti-amyloidogenic activity [59,60]. In addition to their important non-covalent interactions in the anti-amyloidogenic activity, these interactions would increase the nucleophilicity of the terminal amino group and the susceptibility towards a nucleophilic attack at the carbonyl carbon of the *beta*-lactam ring in BP.

BP was found to bind to Aβ and modulate the process of aggregation and toxicity through initial recognition *via* reversible binding interactions (e.g., hydrogen bonding, electrostatic attraction, π-stacking, etc.) followed by covalent bonding between specific functional groups within the Aβ peptide and the *beta*-lactam ring (Fig. 10). The interaction between BP and Aβ involves nucleophilic attack and opening of the *beta*-lactam ring, with the proposed nucleophiles being serine hydroxyl groups, lysine ε-amino groups and the N-terminus of the Aβ peptide.

The biggest challenge in the search for Aβ-aggregation modulator drug candidates is finding molecules that specifically bind to Aβ and inhibit its aggregation. This research may help identify a specific mechanism of interaction with Aβ which may offer scope for structure-based drug design for AD and lead to the development of specific and potent Aβ aggregation modulators. Moreover, the multifunctional properties and safety of *beta*-lactam antibiotics make them promising candidates for clinical trials to treat AD.

Funding

Author contributions

Izzeddin Alsalahat: conception and design of study; acquisition of data; analysis and/or interpretation of data; drafting the manuscript;

revising the manuscript critically for important intellectual content. Zubida M. Al-Majdoub: acquisition of data; analysis and/or interpretation of data. Mutasem O. Taha: acquisition of data; analysis and/or interpretation of data; drafting the manuscript. Jill Barber: revising the manuscript critically for important intellectual content. Harmesh Aojula: revising the manuscript critically for important intellectual content. Nigel Hodson: acquisition of data; analysis and/or interpretation of data. Sally Freeman: conception and design of study; analysis and/or interpretation of data; drafting the manuscript; revising the manuscript critically for important intellectual content. Approval of the version of the manuscript to be published (all authors).

Declaration of competing interest

The authors declare that they have no known competing financial interests or personal relationships that could have appeared to influence the work reported in this paper.

Acknowledgements

Appendix A. Supplementary data

Supplementary data to this article can be found online at https://doi. org/10.1016/j.bbrep.2021.100943.

References

[1] L.C.P. Banning, I.H.G.B. Ramakers, K. Deckers, F.R.J. Verhey, P. Aalten, Apolipoprotein E and affective symptoms in mild cognitive impairment and Alzheimer's disease dementia: a systematic review and meta-analysis, Neurosci. Biobehav. Rev. 96 (2019) 302–315.

[2] K. Blennow, M.J. De Leon, H. Zetterberg, Alzheimer's disease, Lancet 368 (2006) 387–403.

[3] M. Gralle, S.T. Ferreira, Structure and functions of the human amyloid precursor protein: the whole is more than the sum of its parts, Prog. Neurobiol. 82 (2007) 11–32.

[4] G. Thinakaran, E.H. Koo, Amyloid precursor protein trafficking, processing, and function, J. Biol. Chem. 283 (2008) 29615–29619.

[5] R. Sannerud, C. Esselens, P. Ejsmont, R. Mattera, L. Rochin, A.K. Tharkeshwar, G. De Baets, V. De Wever, R. Habets, V. Baert, W. Vermeire, C. Michiels, A.J. Groot, R. Wouters, K. Dillen, K. Vints, P. Baatsen, S. Munck, R. Derua, E. Waelkens, G. S. Basi, M. Mercken, M. Vooijs, M. Bollen, J. Schymkowitz, F. Rousseau, J. S. Bonifacino, G. Van Niel, B. De Strooper, W. Annaert, Restricted location of PSEN2/gamma-secretase determines substrate specificity and generates an intracellular abeta pool, Cell 166 (2016) 193–208.

[6] L. Breydo, D. Kurouski, S. Rasool, S. Milton, J.W. Wu, V.N. Uversky, I.K. Lednev, C. G. Glabe, Structural differences between amyloid beta oligomers, Biochem. Biophys. Res. Commun. 477 (2016) 700–705.

[7] S.J. Roeters, A. Iyer, G. Pletikapić, V. Kogan, V. Subramaniam, S. Woutersen, Evidence for intramolecular antiparallel beta-sheet structure in alpha-synuclein fibrils from a combination of two-dimensional infrared spectroscopy and atomic force microscopy, Sci. Rep. 7 (2017), 41051-41051.

[8] H.M. Wilkins, R.H. Swerdlow, Amyloid precursor protein processing and bioenergetics, Brain Res. Bull. 133 (2017) 71–79.

[9] I. Benilova, E. Karran, B. De Strooper, The toxic Abeta oligomer and Alzheimer's disease: an emperor in need of clothes, Nat. Neurosci. 15 (2012) 349–357.

[10] C. Haass, D.J. Selkoe, Soluble protein oligomers in neurodegeneration: lessons from the Alzheimer's amyloid β-peptide, Nat. Rev. Mol. Cell Biol. 8 (2007) 101–112.

[11] A.J. Doig, M.P. del Castillo-Frias, O. Berthoumieu, B. Tarus, J. Nasica-Labouze, F. Sterpone, P.H. Nguyen, N.M. Hooper, P. Faller, P. Derreumaux, Why is research on amyloid-β failing to give new drugs for Alzheimer's disease? ACS Chem. Neurosci. 8 (2017) 1435–1437.

[12] J. Nasica-Labouze, P.H. Nguyen, F. Sterpone, O. Berthoumieu, N.-V. Buchete, S. Coté, A. De Simone, A.J. Doig, P. Faller, A. Garcia, A. Laio, M.S. Li, S. Melchionna, N. Mousseau, Y. Mu, A. Paravastu, S. Pasquali, D.J. Rosenman, B. Strodel, B. Tarus, J.H. Viles, T. Zhang, C. Wang, P. Derreumaux, Amyloid β protein and Alzheimer's disease: when computer simulations complement experimental studies, Chem. Rev. 115 (2015) 3518–3563.

[13] S. Al-Edresi, I. Alsalahat, S. Freeman, H. Aojula, J. Penny, Resveratrol-mediated cleavage of amyloid β1–42 peptide: potential relevance to Alzheimer's disease, Neurobiol. Aging 94 (2020) 24–33.

[14] A.J. Doig, P. Derreumaux, Inhibition of protein aggregation and amyloid formation by small molecules, Curr. Opin. Struct. Biol. 30 (2015) 50–56.

[15] T. Tomiyama, S. Asano, Y. Suwa, T. Morita, K. Kataoka, H. Mori, N. Endo, Rifampicin prevents the aggregation and neurotoxicity of amyloid beta protein in vitro, Biochem. Biophys. Res. Commun. 204 (1994) 76–83.

[16] B. Yulug, L. Hanoglu, E. Kilic, W.R. Schabitz, RIFAMPICIN: an antibiotic with brain protective function, Brain Res. Bull. 107 (2014) 37–42.

[17] M.B. Loeb, D.W. Molloy, M. Smieja, T. Standish, C.H. Goldsmith, J. Mahony, S. Smith, M. Borrie, E. Decoteau, W. Davidson, A. McDougall, J. Gnarpe, O.M. O'D, M. Chernesky, A randomized, controlled trial of doxycycline and rifampin for patients with Alzheimer's disease, J. Am. Geriatr. Soc. 52 (2004) 381–387.

[18] L. Diomede, G. Cassata, F. Fiordaliso, M. Salio, D. Ami, A. Natalello, S.M. Doglia, A. De Luigi, M. Salmona, Tetracycline and its analogues protect Caenorhabditis elegans from β amyloid-induced toxicity by targeting oligomers, Neurobiol. Dis. 40 (2010) 424–431.

[19] G. Forloni, L. Colombo, L. Girola, F. Tagliavini, M. Salmona, Anti-amyloidogenic activity of tetracyclines: studies in vitro, FEBS Lett. 487 (2001) 404–407.

[20] J. Luo, J.M. Otero, C.H. Yu, S.K. Wärmländer, A. Gräslund, M. Overhand, J. P. Abrahams, Inhibiting and reversing amyloid-β (1-40) fibril formation with gramicidin S and engineered analogues, Chemistry 19 (2013) 17338–17348.

[21] S.K. Chaturvedi, N. Zaidi, P. Alam, J.M. Khan, A. Qadeer, I.A. Siddique, S. Asmat, Y. Zaidi, R.H. Khan, Unraveling comparative anti-amyloidogenic behavior of pyrazinamide and D-cycloserine: a mechanistic biophysical insight, PloS One 10 (2015), e0136528.

[22] S.C. Hartsel, T.R. Weiland, Amphotericin B binds to amyloid fibrils and delays their formation: a therapeutic mechanism? Biochemistry 42 (2003) 6228–6233.

[23] G. Merlini, E. Ascari, N. Amboldi, V. Bellotti, E. Arbustini, V. Perfetti, M. Ferrari, I. Zorzoli, M.G. Marinone, P. Garini, Interaction of the anthracycline 4'-iodo-4'-deoxydoxorubicin with amyloid fibrils: inhibition of amyloidogenesis, Proc. Natl. Acad. Sci. U. S. A. 92 (1995) 2959–2963.

[24] R. Nitrini, The cure of one of the most frequent types of dementia, A Historical Parallel 19 (2005) 156–158.

[25] J. Miklossy, Biology and Neuropathology of Dementia in Syphilis and Lyme Disease, Handbook of Clinical Neurology, Elsevier, Place Published, 2008, pp. 825–844.

[26] G.R. Riviere, K.H. Riviere, K.S. Smith, Molecular and immunological evidence of oral Treponema in the human brain and their association with Alzheimer's disease, Oral Microbiol. Immunol. 17 (2002) 113–118.

[27] M.G. Zagorski, J. Yang, H. Shao, K. Ma, H. Zeng, A. Hong, Methodological and chemical factors affecting amyloid beta peptide amyloidogenicity, Methods Enzymol. 1 (1999) 189–204.

[28] S. Jao, K. Ma, J. Talafous, R. Orlando, M.G. Zagorski, Trifluoroacetic acid pretreatment reproducibly disaggregates the amyloid β-peptide, International Journal of Experimental and Clinical Investigation 4 (1997) 240–252.

[29] N. Kokkoni, K. Stott, H. Amijee, J.M. Mason, A.J. Doig, N-methylated peptide inhibitors of β-amyloid aggregation and toxicity: optimization of the inhibitor structure, Biochemistry 45 (2006) 9906–9918.

[30] F.E. Field, G. Roberts, R.C. Hallowes, A.K. Palmer, K.E. Williams, J.B. Lloyd, Trypan blue: identification and teratogenic and oncogenic activities of its coloured constituents, Chem. Biol. Interact. 16 (1977) 69–88.

[31] K. Abe, N. Matsuki, Measurement of cellular 3-(4,5-dimethylthiazol-2-yl)-2,5-diphenyltetrazolium bromide (MTT) reduction activity and lactate dehydrogenase release using MTT, Neurosci. Res. 38 (2000) 325–329.

[32] W.B. Stine, K.N. Dahlgren, G.A. Krafft, M.J. LaDu, In vitro characterization of conditions for amyloid-β peptide oligomerization and fibrillogenesis, Biol. Chem. 278 (2003) 11612–11622.

[33] E.M. Sigurdsson, Amyloid Proteins: Methods and Protocols, Humana Press Inc., Place Published, 2005.

[34] C.E. Eyers, D.M. Simpson, S.C.C. Wong, R.J. Beynon, S.J. Gaskell, QCAL-a novel standard for assessing instrument conditions for proteome analysis, American Society of Mass Spectrometry (2008) 1275–1280.

[35] M. Feig, C.L. Brooks, Recent advances in the development and application of implicit solvent models in biomolecule simulations, Curr. Opin. Struct. Biol. 14 (2004) 217–224.

[36] G. Wu, D.H. Robertson, C.L. Brooks 3rd, M. Vieth, Detailed analysis of grid-based molecular docking: a case study of CDOCKER-A CHARMm-based MD docking algorithm, J. Comput. Chem. 24 (2003) 1549–1562.

[37] J.D. Harper, P.T. Lansbury, Models of amyloid seeding in Alzheimer's disease and scrapie: mechanistic truths and physiological consequences of the time-dependent solubility of amyloid proteins, Annu. Rev. Biochem. 66 (1997) 385–407.

[38] J. Lu, Q. Cao, C. Wang, J. Zheng, F. Luo, J. Xie, Y. Li, X. Ma, L. He, D. Eisenberg, J. Nowick, L. Jiang, D. Li, Structure-based peptide inhibitor design of amyloid-β aggregation, Front. Mol. Neurosci. 12 (2019).

[39] C. Soto, E.M. Sigurdsson, L. Morelli, R. Asok Kumar, E.M. Castano, B. Frangione, [beta]-sheet breaker peptides inhibit fibrillogenesis in a rat brain model of amyloidosis: implications for Alzheimer's therapy, Nat. Med. 4 (1998) 822–826.

[40] C. Soto, M.S. Kindy, M. Baumann, B. Frangione, Inhibition of alzheimer's amyloidosis by peptides that prevent β-sheet conformation, Biochem. Biophys. Res. Commun. 226 (1996) 672–680.

[41] T. Sato, P. Kienlen-Campard, M. Ahmed, W. Liu, H. Li, J.I. Elliott, S. Aimoto, S. N. Constantinescu, J.N. Octave, S.O. Smith, Inhibitors of amyloid toxicity based on beta-sheet packing of Abeta 40 and Aβ42, Biochemistry 45 (2006) 5503–5516.

[42] R. Khuranaa, C. Colemana, C. Ionescu-Zanettib, S.A. Carterb, V. Krishnac, R. K. Groverd, R. Royd, S. Singhe, Mechanism of Thioflavin T bnding to amyloid fibrils, Struct. Biol. 151 (2005) 229–238.

[43] R.M. Herriott, A spectrophotometric method for the determination OF penicillin, J. Biol. Chem. 164 (1946) 725–736.

[44] T. Kowalewski, D.M. Holtzman, *In situ* atomic force microscopy study of Alzheimer's β-amyloid peptide on different substrates: new insights into mechanism of β-sheet formation, Proc. Natl. Acad. Sci. Unit. States Am. 96 (1999) 3688–3693.

[45] G. Bitan, M.D. Kirkitadze, A. Lomakin, S.S. Vollers, G.B. Benedek, D.B. Teplow, Amyloid β-protein (Aβ) assembly: aβ40 and Aβ42 oligomerize through distinct pathways, Proc. Natl. Acad. Sci. Unit. States Am. 100 (2003) 330–335.

[46] J.D. Harper, S.S. Wong, C.M. Lieber, P.T. Lansbury, Assembly of Aβ amyloid protofibrils:an in vitro model for a possible early event in alzheimer's disease, Biochemistry 38 (1999) 8972–8980.

[47] M. De Ceuleneer, V. De Wit, K. Van Steendam, F. Van Nieuwerburgh, K. Tilleman, D. Deforce, Modification of citrulline residues with 2,3-butanedione facilitates their detection by liquid chromatography/mass spectrometry, Rapid Commun. Mass Spectrom. 25 (2011) 1536–1542.

[48] A. Hassanzadeh, J. Barber, G.A. Morris, P.A. Gorry, Mechanism for the degradation of erythromycin A and erythromycin A 2'-ethyl succinate in acidic aqueous solution, J. Phys. Chem. 111 (2007) 10098–10104.

[49] O. Crescenzi, S. Tomaselli, R. Guerrini, S. Salvadori, A.M. D'Ursi, P.A. Temussi, D. Picone, Solution structure of the alzheimer's disease amyloid beta peptide (1-42), Eur. J. Biochem. 269 (2002) 5642–5648.

[50] D.H. Chui, T. Tabira, S. Izumi, G. Koya, J. Ogata, Decreased beta-amyloid and increased abnormal Tau deposition in the brain of aged patients with leprosy, Am. J. Pathol. 145 (1994) 771–775.

[51] S.B. Socias, F. González-Lizárraga, C.L. Avila, C. Vera, L. Acuña, J.E. Sepulveda-Diaz, E. Del-Bel, R. Raisman-Vozari, R.N. Chehin, Exploiting the therapeutic potential of ready-to-use drugs: repurposing antibiotics against amyloid aggregation in neurodegenerative diseases, Prog. Neurobiol. 162 (2018) 17–36.

[52] J. Wei, X. Pan, Z. Pei, W. Wang, W. Qiu, Z. Shi, G. Xiao, The beta-lactam antibiotic, ceftriaxone, provides neuroprotective potential via anti-excitotoxicity and anti-inflammation response in a rat model of traumatic brain injury, The journal of trauma and acute care surgery 73 (2012) 654–660.

[53] Y. Gu, C. Walker, M.E. Ryan, J.B. Payne, L.M. Golub, Non-antibacterial tetracycline formulations: clinical applications in dentistry and medicine, J. Oral Microbiol. 4 (2012) 19227.

[54] C. Walker, P.M. Preshaw, J. Novak, A.F. Hefti, M. Bradshaw, C. Powala, Long-term treatment with sub-antimicrobial dose doxycycline has no antibacterial effect on intestinal flora, J. Clin. Periodontol. 32 (2005) 1163–1169.

[55] R.A. Ashley, Clinical trials of a matrix metalloproteinase inhibitor in human periodontal disease. SDD Clinical Research Team, Ann. N. Y. Acad. Sci. 878 (1999) 335–346.

[56] W.V. Giannobile, Host-response therapeutics for periodontal diseases, J. Periodontol. 79 (2008) 1592–1600.

[57] T.R. Jahn, O.S. Makin, K.L. Morris, K.E. Marshall, P. Tian, P. Sikorski, L.C. Serpell, The common architecture of cross-β amyloid, J. Mol. Biol. 395 (2010) 717–727.

[58] M. Sunde, L.C. Serpell, M. Bartlam, P.E. Fraser, M.B. Pepys, C.C. Blake, Common core structure of amyloid fibrils by synchrotron X-ray diffraction, J. Mol. Biol. 273 (1997) 729–739.

[59] U. Cosentino, D. Pitea, G. Moro, G.A.A. Saracino, P. Caria, R.M. Varì, L. Colombo, G. Forloni, F. Tagliavini, M. Salmona, The anti-fibrillogenic activity of tetracyclines on PrP 106–126: a 3D-QSAR study, J. Mol. Model. 14 (2008) 987–994.

[60] K. Pyta, P. Przybylski, K. Klich, J. Stefańska, A new model of binding of rifampicin and its amino analogues as zwitterions to bacterial RNA polymerase, Org. Biomol. Chem. 10 (2012) 8283–8297.